DALTON

Synthetic, structural, electrochemical and electronic characterisation of heterobimetallic bis(acetylide) ferrocene complexes

Michael C. B. Colbert,[a] **Jack Lewis,**[a] **Nicholas J. Long,***[b] **Paul R. Raithby,**[a] **Andrew J. P. White**[b] **and David J. Williams**[b]

[a] *Department of Chemistry, University of Cambridge, Lensfield Road, Cambridge CB2 1EW, UK*
[b] *Department of Chemistry, Imperial College of Science, Technology and Medicine,*
South Kensington, London SW7 2AY, UK

A series of novel heterobimetallic bis(acetylide) ferrocene complexes featuring a bis[1,2-bis(diphenylphosphino)-methane]ruthenium centre and seven variously substituted aromatic acetylene ligands have been synthesised and characterised. The crystal structure of *trans*-[Ru(dppm)$_2${C≡C(C$_5$H$_4$)Fe(C$_5$H$_5$)}$_2$] shows the ruthenium centre in a distorted-octahedral environment bound to two ferrocene units in a linear fashion by 'rigid-rod'-like acetylene linkages. The conformation is stabilised by strong intramolecular CH···π(C≡C) interactions. Electrochemical studies showed that incorporation of donor-substituted aromatic acetylide ligands causes a cathodic shift in the Ru$^{II/III}$ redox potential. Conversely, an anodic shift is observed when electron-withdrawing substituents are present in the acetylide systems. Electronic spectral measurements indicated that the systems belong to the Robin and Day 'Class II' mixed-valence species and suggest that greater electronic interaction occurs in the bis(acetylide) complexes than in the corresponding monoacetylide chloro-complex.

Ferrocene-containing complexes are currently receiving much attention due to their increasing role in the rapidly growing area of materials science. Metallocenes and, in particular ferrocene, have been of use as molecular ferromagnets,[1,2] molecular sensors,[3,4] electrochemical agents[5] and in non-linear optics.[6,7] Increasing demand for new materials for the development of optoelectronic technology has encouraged us to design new systems featuring 'donor–acceptor' and 'long-chain' π-delocalised characteristics which might exhibit properties essential for second- and third-order non-linear optical phenomena.[6,8–10] Introduction of another metal in close proximity to the metallocenyl complex gives a wider diversity of oxidation states and ligands which increases the possible architectural flexibility and fine-tuning of the properties essential for device application.

Following our initial reports of the synthesis and characterisation of ruthenium and osmium complexes of ferrocenylacetylene,[11] we have expanded this system by incorporation of a second acetylene ligand, to form some novel bis(acetylide) complexes of ruthenium.

Results and Discussion

(*a*) Synthesis

An expansion of our previously reported ferrocenyl metal–acetylide systems was accomplished through substitution of the chlorine atom in the complex [(C$_5$H$_5$)Fe^{II}(C$_5$H$_4$)C≡CRu^{II}(dppm)$_2$Cl] **1a** by a second acetylene ligand, yielding complexes of the type [(C$_5$H$_5$)Fe^{II}(C$_5$H$_4$)C≡CRu^{II}(dppm)$_2$(C≡CR)] **2a**–**2g** (Scheme 1). The synthetic route was modified from a literature procedure.[12] The substitution of the chloride was concomitant with a change of electron density on the ruthenium centre with respect to **1a**; the shift in electrode potentials ($E_{\frac{1}{2}}$) of the Ru$^{II/III}$ redox couple in the system was then used as an indication of this electron-density change. Electrochemical experiments indicated that the complexes could be further converted by chemical means to a mixed-valence form [(C$_5$H$_5$)Fe^{III}(C$_5$H$_4$)C≡CRu^{II}(dppm)$_2$(C≡CR)][PF$_6$] by reaction with ferrocenium hexafluorophosphate (Scheme 3, see later).

The reactions in Scheme 1 were monitored by IR spectroscopy, there being a distinct change in the ν(C≡C) stretching frequency in going from complex **1a** to **2a**–**2g**. Complexes

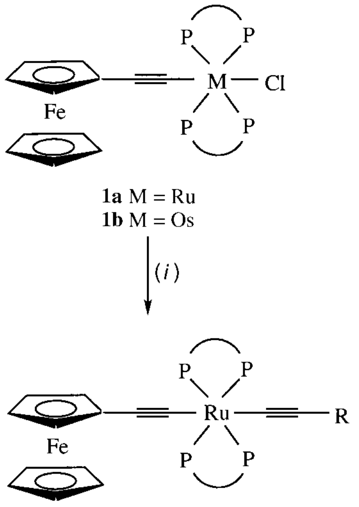

2a–2g

R = Ph **a**, C$_6$H$_4$Ph-4 **b**, C$_6$H$_4$Me-4 **c**, C$_6$H$_4$NO$_2$-4 **d**, C$_6$H$_3$Me-3-NO$_2$-4 **e**, C$_6$H$_4$NO$_2$-2 **f**, or ferrocenyl **g**

Scheme 1 P–P = 1,2-Bis(diphenylphosphino)methane (dppm). (*i*) NaPF$_6$ (1 equivalent), HC≡CR (1 equivalent), NEt$_3$ (2 equivalents), **1a** (1 equivalent), CH$_2$Cl$_2$, 24 h, room temperature (r.t.), N$_2$

2a–**2g** were purified using an alumina chromatography column and CH$_2$Cl$_2$ as eluent. They were isolated in yields ranging from 20 to 50%, **2a**–**2c**, **2g** being orange-yellow powders, whilst **2d**–**2f** were red. Each complex was recrystallised from CH$_2$Cl$_2$–diethyl ether or hexane two-layered systems and the resulting crystals were found analytically to contain half a molecule of CH$_2$Cl$_2$ per mol of complex. Crystals of **2g** suitable for single-crystal X-ray analysis were isolated from slow evaporation of a concentrated CH$_2$Cl$_2$ solution.

(*b*) Crystal structure

The structure of complex **2g** is shown in Fig. 1 whilst selected bond parameters are listed in Table 1. {The structure of the analogous monoacetylide osmium precursor [(C$_5$H$_5$)Fe(C$_5$H$_4$)-

Table 1 Selected bond lengths (Å) and angles (°) for complex **2g**

Ru–C(1)	2.072(4)	Ru–P(14)	2.3192(12)
Ru–P(28)	2.3333(12)	C(1)–C(2)	1.199(6)
C(2)–C(3)	1.432(6)	C(3)–C(4)	1.430(6)
C(3)–C(7)	1.442(7)	C(3)–Fe(8)	2.074(4)
C(4)–C(5)	1.417(7)	C(4)–Fe(8)	2.038(4)
C(5)–C(6)	1.394(8)	C(5)–Fe(8)	2.019(5)
C(6)–C(7)	1.412(7)	C(6)–Fe(8)	2.025(5)
C(7)–Fe(8)	2.045(5)	Fe(8)–C(11)	2.031(5)
Fe(8)–C(10)	2.034(5)	Fe(8)–C(12)	2.037(5)
Fe(8)–C(9)	2.041(5)	Fe(8)–C(13)	2.050(5)
C(9)–C(13)	1.411(7)	C(9)–C(10)	1.424(7)
C(10)–C(11)	1.391(8)	C(11)–C(12)	1.425(8)
C(12)–C(13)	1.408(7)	P(14)–C(27)	1.856(4)
C(27)–P(28)	1.851(4)		
C(1)–Ru–C(1A)	180.0	C(1)–Ru–P(14A)	85.04(12)
C(1)–Ru–P(14)	94.96(12)	P(14A)–Ru–P(14)	180.0
C(1)–Ru–P(28A)	80.96(12)	P(14)–Ru–P(28A)	108.63(4)
C(1)–Ru–P(28)	99.04(12)	P(14)–Ru–P(28)	71.37(4)
P(28A)–Ru–P(28)	180.0	C(2)–C(1)–Ru	174.0(4)
C(1)–C(2)–C(3)	174.7(5)	C(4)–C(3)–C(2)	128.7(4)
C(4)–C(3)–C(7)	106.1(4)	C(2)–C(3)–C(7)	125.1(4)
C(5)–C(4)–C(3)	108.4(5)	C(6)–C(5)–C(4)	108.6(4)
C(5)–C(6)–C(7)	108.6(5)	C(6)–C(7)–C(3)	108.3(5)
C(13)–C(9)–C(10)	108.2(5)	C(11)–C(10)–C(9)	108.3(5)
C(10)–C(11)–C(12)	107.7(5)	C(13)–C(12)–C(11)	108.6(5)
C(9)–C(13)–C(12)	107.3(5)	C(27)–P(28)–Ru	93.80(14)
C(27)–P(14)–Ru	94.1(2)	P(28)–C(27)–P(14)	94.1(2)

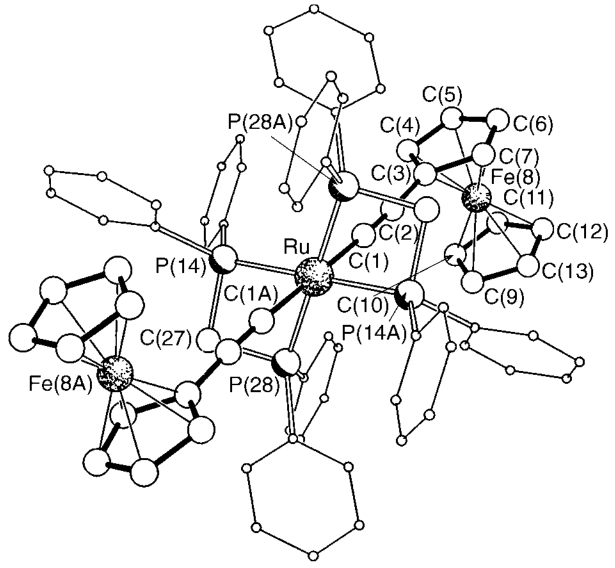

Fig. 1 Perspective view of the structure of complex **2g**

C≡COs(dppm)$_2$Cl] has been reported previously.[11]} The determination confirmed **2g** to have the desired constitution, with ethynylferrocene units in *trans* positions with respect to the ruthenium centre. The complex has crystallographic C_i symmetry and the ruthenium atom has a distorted-octahedral geometry with *cis* angles at Ru in the range 71.4(1)–108.6(1)°. These distortions are a consequence of the 'bite angle' of the chelating phosphine. The axial ruthenium–acetylide bonds are slightly inclined, by 81°, to the phosphorus-containing equatorial co-ordination plane. The Ru–P distances are typical at 2.319(1) and 2.333(1) Å, whilst the Ru–C distances of 2.072(4) Å and the C≡C bond lengths of 1.199(6) Å, are characteristic of a ruthenium σ bonded to an ethynylic function.[13,14] The Ru–C–C≡C chain is almost linear, with angles at C(1) and C(2) of 174.0(4) and 174.7(5)° respectively. There is also adoption of a conventional, parallel, eclipsed geometry by the ferrocenyl unit. Another notable feature of the molecule is the directing of one of the *ortho* C–H groups of one of the phosphine phenyl rings towards the centre of the π system of the ethyne bond (Fig. 2). The H···π system distance is 2.51 Å and the C–H···π system angle is 160°, indicative of a strong interaction.[15] The H···π system bond is inclined by 80° to the C(1)–C(2) triple bond.

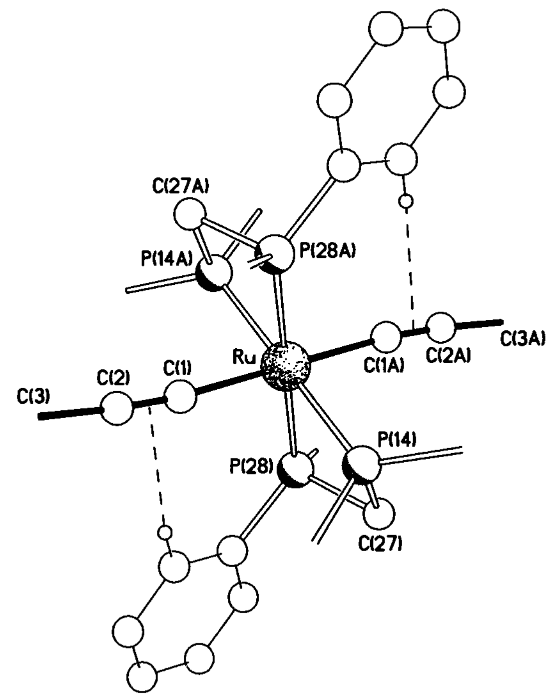

Fig. 2 The CH ··· π system stabilising interactions in the structure of complex **2g**; ferrocenyl and non-interacting phenyl components have been omitted for clarity

Interestingly, inspection of the crystal packing reveals the presence of channels bounded by the phosphine rings that run in the crystallographic *a* direction. The channels have an approximately square cross-section with a mean-free pathway of *ca.* 5 Å. The crystal packing is centrosymmetric (*Pnaa*) thus precluding any second-order non-linear optical activity. However, it was hoped that this and the other bis(acetylide) analogues could act as precursors for long-chain π-delocalised ferrocenyl metal–acetylide oligo- and poly-meric systems and that their electrochemical behaviour and spectrochemical properties might provide greater insight into the nature of the metal–ligand interactions.

(*c*) Electrochemistry

The electrochemistry of the bis(acetylide) complexes **2a**–**2g** was carried out at 298 K in a standard three-electrode system (platinum working/auxiliary electrode and silver-wire reference electrode) using a 0.1 mol dm^{-3} [NBu$^n_4$][BF$_4$]–CH$_2$Cl$_2$ solution as electrolyte and the results of the voltammetric experiments are in Table 2.

The quasi-reversible nature of the metal redox potentials was confirmed by standard diagnostic tests, *e.g.* (*i*) $\Delta E_p = 0.06–0.10$ V and (*ii*) $i_{pc}/i_{pa} = 1$ with varying scan rates from 0.05 to 0.5 V s^{-1}. The changes in the relative $E_{\frac{1}{2}}$ values compared with complex **1a** were very evident. Replacement of the chloride atom in **1a** by the donor ligands **a**–**c** caused a cathodic shift in the Ru$^{II/III}$ redox potential while the opposite can be stated for the electron-withdrawing ligands **d**–**g**. The iron $E_{\frac{1}{2}}$ values were not greatly affected by the ligand substitution. The ΔE_p values of complexes **2a**–**2g** were lower than that of **1a** suggesting that the rate of electron transfer to the electrode from the Fe^{II}Ru^{II} metal centres in the bis(acetylide) system is greater than in the *trans*-ferrocenyl metal chloride complexes.

The cyclic voltammogram of complex **2g** (Fig. 3) displayed three chemically reversible oxidation processes [$E_{\frac{1}{2}} = 0.45$ (III), −0.18 (II) and −0.40 V (I)]. The least anodic processes were a

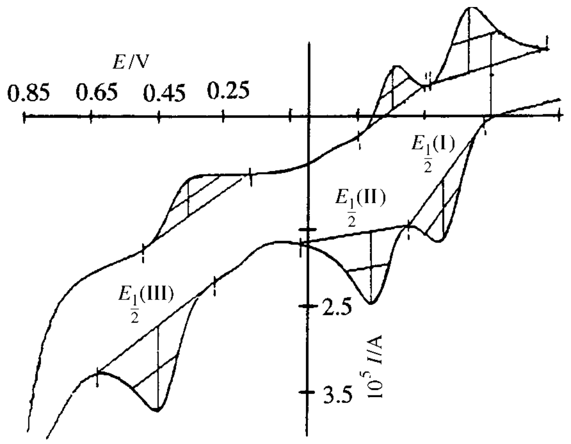

Fig. 3 Cyclic voltammogram of complex **2g**

$$\mathrm{Fe^{II}{-}Ru^{II}{-}Fe^{II}} \underset{+e^-}{\overset{-e^-}{\rightleftharpoons}} \mathrm{Fe^{III}{-}Ru^{II}{-}Fe^{II}} \underset{+e^-}{\overset{-e^-}{\rightleftharpoons}}$$

Yellow Blue

$$\mathrm{Fe^{III}{-}Ru^{II}{-}Fe^{III}} \underset{+e^-}{\overset{-e^-}{\rightleftharpoons}} \mathrm{Fe^{III}{-}Ru^{III}{-}Fe^{III}}$$

Violet Purple

Scheme 2

multiwave system separated by 0.22 V ($K_c = 5 \times 10^{-3}$), which can clearly be assigned to the two iron centres interacting with each other through the acetylide ruthenium bridge (C≡C–Ru–C≡C).

These assignments would suggest that replacement of the chloride ligand on the ruthenium centre by the ferrocenylacetylide ligand anodically shifts the $\mathrm{Ru^{II/III}}$ redox potential. This is supported by electrochemical studies on analogous ruthenium ferrocenylacetylide complexes.[16] This conclusion is in contradiction to our previous publication[11] featuring complexes **1a** and **1b** where the assignment of the redox potentials was based on electrochemical experiments conducted on complexes of the type $[\mathrm{Ru(dppm)_2(C{\equiv}CR)_{2-\mathit{n}}Cl_{\mathit{n}}}]$ (n = 0 or 1).[13c] The latter experiments suggested that replacement of one chloride ligand by an arylacetylide cathodically shifts the $\mathrm{Ru^{II/III}}$ redox potential.

Coulometry experiments on complex **2g** showed that each redox process involved one-electron transfer. The products of each oxidation step had distinct colours associated with mono- and di-cationic species (and in the case of **2g**, a tricationic complex). An overall mechanism for the electron-transfer processes occuring in complex **2g** is shown in Scheme 2.

The electrochemical behaviour of these systems was greatly affected by the degree of metal–metal interaction, and it was found that $\Delta E_{\frac{1}{2}}$ values [and corresponding α^2 values, see section (*d*)] for a specific system were greater as the delocalisation between the metal centres increased. However, the $\Delta E_{\frac{1}{2}}$ values cannot be used to evaluate directly the degree of metal–metal interaction in these asymmetric systems since $\Delta E_{\frac{1}{2}}$ is caused by a combination of the inherent differences in redox potentials of the metal sites and to a lesser extent by a degree of metal–metal interaction.

(*d*) Electronic spectra

Chemical oxidation of complexes **2a**–**2d** and **2g** with ferrocenyl hexafluorophosphate (Scheme 3) led to the isolation of the mixed-valence analogues $\mathbf{2a^+}$–$\mathbf{2d^+}$ and $\mathbf{2g^+}$ as air-stable purple powders in high yields (90%). The IR spectra of the mixed-valence complexes showed two absorptions at *ca.* 2070w and *ca.* 1985s $\mathrm{cm^{-1}}$ which were assigned as ν(C≡C) and ν(M=C=C=C) stretching frequencies (Scheme 4).

Electrochemical experiments indicated that complexes $\mathbf{2a^+}$–$\mathbf{2d^+}$ and $\mathbf{2g^+}$ were stable in solution and could be analysed by spectroscopy. Their electronic spectra contained an intervalence charge-transfer (i.v.c.t.) band in the near-IR region at *ca.* 1500 nm and two bands at *ca.* 450 and 580 nm in the UV region (Fig. 4). The relevant data from the spectra are detailed in Table 3.

The spectroscopic data were treated using Hush theory

Table 2 Electrochemical data for the ruthenium bis(acetylide) complexes

Complex	$E_{\frac{1}{2}}(\mathrm{Fe^{II/III}})$/ V	ΔE_p (Fe)/ V	$E_{\frac{1}{2}}(\mathrm{Ru^{II/III}})$/ V	ΔE_p (Ru)/ V	$\Delta E_{\frac{1}{2}}$/ V
1a	−0.39	0.14	0.37	0.15	0.76
2a	−0.34	0.08	0.22	0.08	0.56
2b	−0.33	0.08	0.19	0.10	0.52
2c	−0.32	0.07	0.20	0.06	0.52
2d	−0.30	0.10	0.34	0.08	0.64
2e	−0.29	0.07	0.33	0.06	0.62
2f	−0.29	0.07	0.33	0.07	0.62
2g	−0.18, −0.40	0.07	0.45	0.09	0.63, 0.85

All $E_{\frac{1}{2}}$ were referenced to ferrocene in the same system, scan rate 100 mV $\mathrm{s^{-1}}$; $\Delta E_{\frac{1}{2}} = E_{\frac{1}{2}(\mathrm{Ru})} - E_{\frac{1}{2}(\mathrm{Fe})}$.

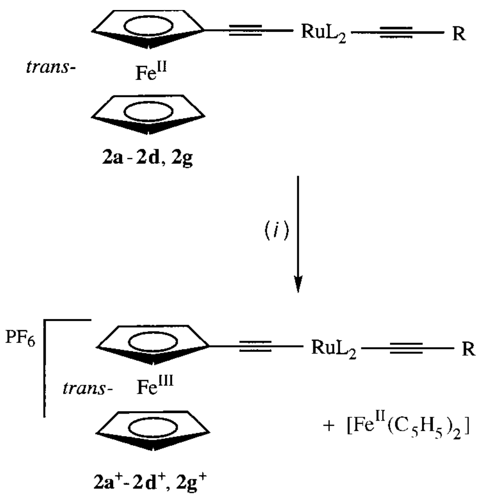

Scheme 3 L = dppm. (*i*) Ferrocenium hexafluorophosphate, $\mathrm{CH_2Cl}$, 0 °C, 20 min

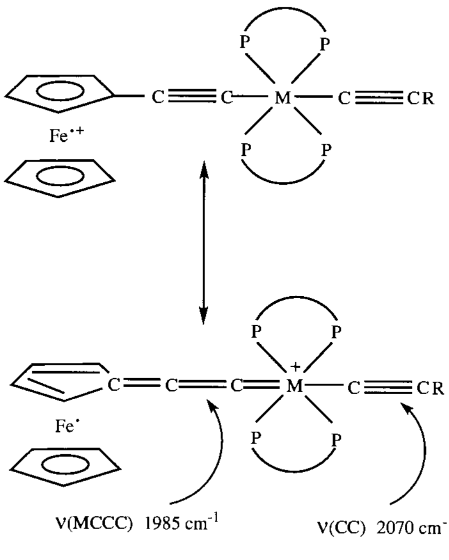

Scheme 4 Schematic diagram of the bis(acetylide) mixed-valence complexes

Table 3 Electronic absorption energies and related data for the oxidised bis(acetylide) $Fe^{III}Ru^{II}$ complexes

Complex	UV λ/nm	$\tilde{\nu}_{max}/cm^{-1}$	$\Delta\nu_{\frac{1}{2}}/cm^{-1}$	$\Delta E_{\frac{1}{2}}/V$	$\nu_{0(calc.)}/cm^{-1}$	$\Delta\nu_{\frac{1}{2}(calc.)}/cm^{-1}$	$10^3\ \alpha^2$
2a$^+$	439, 592	6610	1780	0.56	4480	2218	4.8
2b$^+$	433, 592	6560	1934	0.52	4160	2355	3.7
2c$^+$	445, 578	6555	1932	0.52	4160	2352	3.8
2d$^+$	None	6655	2149	0.64	5120	1883	6.9
2g$^+$	447, 610	6760	1268	0.63	5040	1993	6.2

When $\Delta E_{\frac{1}{2}} = 0.1$ V then $\nu_0 = 800\ cm^{-1}$; *r*, the distance from ruthenium to iron, was taken as 6.7 Å.

Table 4 Electronic absorbance energies and related data for the oxidised ferrocenyl monoacetylide chlorides of Ru and Os

Complex	UV λ/nm	$\tilde{\nu}_{max}/cm^{-1}$	$\Delta\nu_{\frac{1}{2}}/cm^{-1}$	$\Delta E_{\frac{1}{2}}/V$	$\nu_{0(calc.)}/cm^{-1}$	$\Delta\nu_{\frac{1}{2}(calc.)}/cm^{-1}$	$10^3\ \alpha^2$
1a$^+$	438, 600	6570	1982	0.70	5600	1496	3.1
1b$^+$	463, 610	6864	2172	0.65	5200	1960	3.0

r, The distance from the Ru or Os metal to the centroid of the $C_5H_4(C{\equiv}C)$ ring, is *ca.* 6.3 Å.

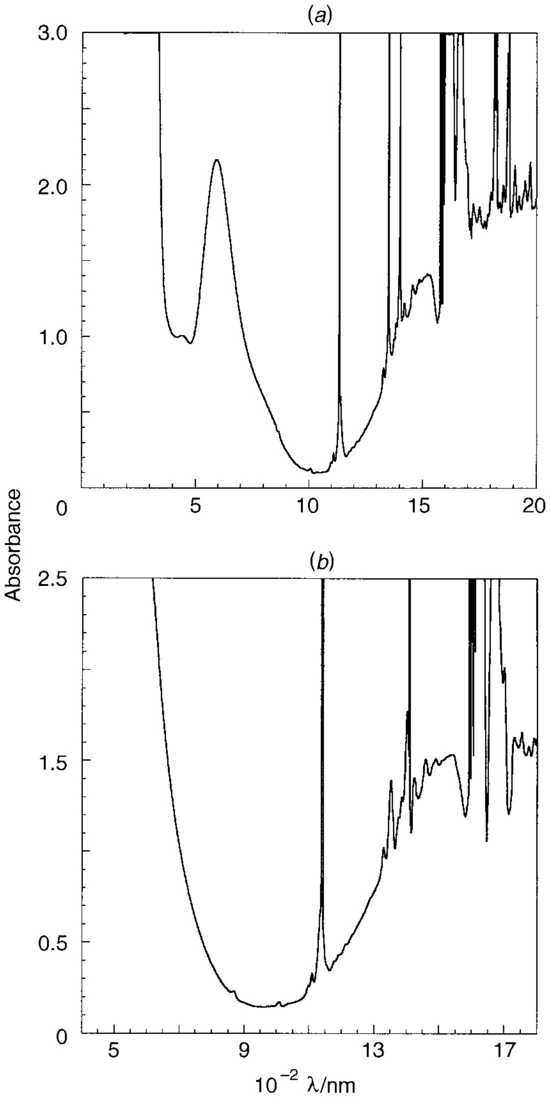

Fig. 4 Electronic spectra of (*a*) $[(C_5H_5)Fe^{III}(C_5H_4)C{\equiv}CRu^{II}L_2(C{\equiv}CPh)][PF_6]$ and (*b*) $[(C_5H_5)Fe^{III}(C_5H_4)C{\equiv}CRu^{II}L_2(C{\equiv}CC_6H_4NO_2\text{-}4)][PF_6]$ (L = dppm)

equations (1) and (2) and permitted the 'mixed-valence

$$\nu_{max} - \nu_0 = (\Delta\nu_{\frac{1}{2}})^2/2310\ (cm^{-1}) \qquad (1)$$

$$\alpha^2 = [(4.2 \times 10^{-4})\varepsilon_{max}\Delta\nu_{\frac{1}{2}}]/\nu_{max}r^2 \qquad (2)$$

classification' of the complexes (ν_0 is the internal energy difference between the two oxidation-state isomers, α^2 = delocalisation parameter, *r*/Å = distance between the metals and $\varepsilon_{max}/dm^3\ mol^{-1}\ cm^{-1}$ = molar absorption coefficient). According to Taube's treatment of oxidised $[(C_5H_5)Fe(C_5H_4)CNRu(NH_3)_5]$,[17] an upper limit to the value of ν_0 (Δ*G*) can be estimated from the difference in the redox potentials ($\Delta E_{\frac{1}{2}}$) of the two metal centres ($\Delta E_{\frac{1}{2}}$ of 0.1V corresponds to a ν_0 value of *ca.* $8 \times 10^2\ cm^{-1}$).

The ratio of the observed and calculated $\Delta\nu_{\frac{1}{2}}$ values ranges from 0.6 to 1.1, the latter being in agreement with the values calculated for the ferrocenyl monoacetylide ruthenium and osmium complexes (Table 4).[18]

The results of the Hush treatment show the ratio of the $\Delta\nu_{\frac{1}{2}(obs)}$ and $\Delta\nu_{\frac{1}{2}(calc)}$ values to be 1.3 and 1.1 for complexes **1a**$^+$ and **1b**$^+$ respectively. These ratios are in better agreement, compared to those measured for the ferrocenylmanganese systems, with the mixed-valence complexes of Class II systems previously reported.[19] The corresponding α^2 values also indicate that the electronic coupling is greater than for the previously measured ferrocenylmanganese complexes;[20] this suggests that **1a**$^+$ and **1b**$^+$ are more strongly delocalised 'Class II' systems.

The α^2 delocalisation parameter calculated for the bis(acetylide) mixed-valence species **2a**$^+$–**2d**$^+$ and **2g**$^+$ indicates that once again the systems belong to Robin and Day 'Class II' mixed-valence species, and the values were larger than those measured for the *trans*-ferrocenyl–metal chloride systems **1a**$^+$ and **1b**$^+$ (Table 4). This means that replacement of the Cl ligand *trans* to the ferrocenyl ligand by another acetylene group allows for more electronic interaction and delocalisation between the two metal centres.

For more details on the elucidation of the properties of mixed-valence complexes and an understanding of the physical properties of these materials with respect to electron-transfer reactions in solutions, see refs. 21–23.

Experimental

General

All preparations were carried out using standard Schlenk techniques.[24] All solvents were distilled over standard drying agents under nitrogen directly before use and all reactions were carried out under an atmosphere of nitrogen. Alumina gel (type UG-1) and silica gel (230–400 mesh) were used for chromatographic separations.

All NMR spectra were recorded on Bruker instruments, operating at either 250 or 400 MHz. Chemical shifts are reported in δ using $CDCl_3$ (^1H, δ 7.25; ^{13}C, δ 77.0) as the reference for ^1H and $^{13}C\text{-}\{^1H\}$ spectra, while the $^{31}P\text{-}\{^1H\}$ spectra were referenced to trimethyl phosphite. The IR spectra were recorded using NaCl solution cells (CH_2Cl_2) using a Perkin-Elmer 1710 Fourier-transform spectrometer, mass spectra using positive FAB methods on a Kratos MS60 spectrometer and electronic spectra in solution cells (CH_2Cl_2) on a Perkin-Elmer Lambda 9 UV/NIR spectrometer. Microanalyses were carried out at the Department of Chemistry, University of Cambridge. The electrochemistry was recorded using an Autolab PGSTAT 20 potentiostat with a standard three-electrode system (platinum working/auxiliary electrodes and silver-wire reference electrode). The experiments were performed at 298 K using a 0.1 mol dm^{-3} $[NBu^n_4][BF_4]$–CH_2Cl_2 (solvent dried over CaH_2) solution as supporting electrolyte and all solutions were purged with N_2. All measurements were referenced using internal ferrocene ($E_{\frac{1}{2}} = 0.0$ V at 298 K in 0.1 mol dm^{-3} $[NBu^n_4][BF_4]$–CH_2Cl_2).

X-Ray crystallography

Crystal data. $C_{74}H_{62}Fe_2P_4Ru$ **2g**, $M = 1287.9$, orthorhombic, space group *Pnaa* (non-standard setting of *Pccn*, number 56), $a = 9.730(3)$, $b = 25.155(2)$, $c = 26.850(2)$ Å, $U = 6572(2)$ Å^3, $Z = 4$ (the molecule has crystallographic C_i symmetry), $D_c = 1.30$ g cm^{-3}, Mo-Kα radiation, $\lambda = 0.710\,73$ Å, μ(Mo-Kα) = 8.0 cm^{-1}, $F(000) = 2648$. Orange-red block, crystal dimensions 0.53 × 0.30 × 0.23 mm.

Data collection and processing. Data were measured on a Siemens P4/PC diffractometer with Mo-Kα radiation (graphite monochromator) using ω scans. 5784 Independent reflections were measured ($2\theta \leqslant 50°$) of which 3871 had $|F_o| > 4\sigma(|F_o|)$ and were considered observed; the data were corrected for Lorentz-polarisation factors but not for absorption.

Structure analysis and refinement. The structure was solved by direct methods and the non-hydrogen atoms were refined anisotropically (phenyl rings being treated as optimised rigid bodies). The positions of the hydrogen atoms were idealised, assigned isotropic thermal parameters, $U(H) = 1.2U_{eq}(C)$, and allowed to ride on their parent carbon atoms. Refinement was by full-matrix least squares based on F^2 to give $R1 = 0.048$, $wR2 = 0.118$ for the observed data and 319 parameters $[w^{-1} = \sigma^2(F_o^2) + (aP)^2 + (bP)]$. The maximum and minimum residual electron densities in the final ΔF map were 0.40 and −0.28 e Å^{-3} respectively. The mean and maximum shift/error ratios in the final refinement cycle were 0.004 and −0.032 respectively.

Computations were carried out on a 50 MHz 486 computer using the SHELXTL PC program system.[25] Atomic coordinates, thermal parameters, and bond lengths and angles have been deposited at the Cambridge Crystallographic Data Centre (CCDC). See Instructions for Authors, *J. Chem. Soc., Dalton Trans.*, 1997, Issue 1. Any request to the CCDC for this material should quote the full literature citation and the reference number 186/287.

Synthesis of heterobimetallic bis(acetylide) ferrocenyl complexes

Complexes **2a**–**2g** were formed from the ferrocenyl ruthenium complex **1a**.[11] They were synthesised using the following two general methods, both adapted from literature procedures.[26]

***trans*-[(C₅H₅)Fe(C₅H₄)C≡CRu(dppm)₂(C≡CR)] 2a–2c, 2g.** A solution of NEt_3 (0.62 mmol) and acetylide **a–c, g** (0.31 mmol) in CH_2Cl_2 (20 cm^3) was added to *trans*-$[(C_5H_5)Fe(C_5H_4)C{\equiv}CRu(dppm)_2Cl]$ (0.35 g, 0.31 mmol) and $NaPF_6$ (0.05 g, 0.31 mmol) also in CH_2Cl_2 (20 cm^3). This mixture was left to stir for 20 h in the absence of light. Addition of one drop of 1,8-diazabicyclo[5.4.0]undec-7-ene (dbu) and 1 h further stirring ensured completion of reaction. There was a slight darkening of the solution over this time and a significant change in the IR ν(C≡C) stretching frequency. The solution was then filtered and the solvent removed *in vacuo*. The resultant dark solid was washed with acetone and filtered, yielding a fine yellow powder of *trans*-$[(C_5H_5)Fe(C_5H_4)C{\equiv}CRu(dppm)_2(C{\equiv}CR)]$ (0.14 mmol, 45%). This powder could be further purified by recrystallisation from a CH_2Cl_2–hexane two-layered system.

trans-$[(C_5H_5)Fe(C_5H_4)C{\equiv}CRu(dppm)_2(C{\equiv}CPh)]$ **2a** (Found: C, 69.9; H, 4.8. $C_{70}H_{57}FeP_4Ru{\cdot}0.5CH_2Cl_2$ requires C, 69.3; H, 4.7%): $\tilde{\nu}$/cm^{-1} (CH_2Cl_2) 2070 (C≡C); $\delta_H(CDCl_3)$ 3.52 (2 H, t), 3.71 (5 H, s), 3.80 (2 H, t), 4.80 (4 H, m) and 6.3–7.6 (45 H, m); $\delta_P(CDCl_3)$ −144.6; $\delta_C(CDCl_3)$ 52.0 (CH_2 of dppm), 65.4, 68.7, 68.9 (ferrocenyl C), 109, 115 (C≡C) and 122–136 (Ph of dppm); *m/z* 1180 (M^+).

trans-$[(C_5H_5)Fe(C_5H_4)C{\equiv}CRu(dppm)_2(C{\equiv}CC_6H_4Ph\text{-}4)]$ **2b** (Found: C, 70.7; H, 4.8. $C_{76}H_{61}FeP_4Ru{\cdot}0.5CH_2Cl_2$ requires C, 70.7; H, 4.7%): $\tilde{\nu}$/cm^{-1} (CH_2Cl_2) 2068 (C≡C); $\delta_H(CDCl_3)$ 3.52 (2 H, t), 3.71 (5 H, s), 3.80 (2 H, t), 4.80 (4 H, m) and 6.3–7.6 (49 H, m); $\delta_P(CDCl_3)$ −144.8; $\delta_C(CDCl_3)$ 52.0 (CH_2 of dppm), 65.4, 68.7, 68.9 (ferrocenyl C), 109, 112 (C≡C) and 122–136 (Ph of dppm); *m/z* 1256.4 (M^+).

trans-$[(C_5H_5)Fe(C_5H_4)C{\equiv}CRu(dppm)_2(C{\equiv}CC_6H_4Me\text{-}4)]$ **2c** (Found: C, 70.9; H, 4.8. $C_{71}H_{59}FeP_4Ru$ requires C, 71.5; H, 4.9%): $\tilde{\nu}$/cm^{-1} (CH_2Cl_2) 2071 (C≡C); $\delta_H(CDCl_3)$ 2.17 (3 H, s), 3.51 (2 H, t), 3.71 (5 H, s), 3.80 (2 H, t), 4.82 (4 H, m) and 6.3–7.6 (44 H, m); $\delta_P(CDCl_3)$ −144.7; $\delta_C(CDCl_3)$ 18.1 (C_6H_4*Me*), 52.0 (CH_2 of dppm), 65.4, 68.7, 68.9 (ferrocenyl C), 109, 114 (C≡C) and 122–136 (Ph of dppm); *m/z* 1194.6 (M^+).

trans-$[Ru(dppm)_2\{C{\equiv}C(C_5H_4)Fe(C_5H_5)\}_2]$ **2g** (Found: C, 67.3; H, 4.8. $C_{74}H_{62}Fe_2P_4Ru{\cdot}0.5CH_2Cl_2$ requires C, 67.1; H, 4.7%): $\tilde{\nu}$/cm^{-1} (CH_2Cl_2) 2072 (C≡C); $\delta_H(CDCl_3)$ 3.51 (4 H, t), 3.71 (10 H, s), 3.80 (4 H, t), 4.80 (4 H, m) and 7.1–7.6 (40 H, m); $\delta_P(CDCl_3)$ −144.6; $\delta_C(CDCl_3)$ 52.4 (CH_2 of dppm), 65.3, 68.7, 68.9 (ferrocenyl C), 108 (C≡C) and 122–136 (Ph of dppm); *m/z* 1289.0 (M^+).

***trans*-[(C₅H₅)Fe(C₅H₄)C≡CRu(dppm)₂(C≡CR)] 2d–2f.** A solution of NEt_3 (0.62 mmol) and acetylide **d–f** (0.31 mmol) in CH_2Cl_2 (20 cm^3) was added to *trans*-$[(C_5H_5)Fe(C_5H_4)C{\equiv}CRu(dppm)_2Cl]$ (0.35 g, 0.31 mmol) and $NaPF_6$ (0.05 g, 0.31 mmol) also in CH_2Cl_2 (20 cm^3). This mixture was left to stir for 20 h in the absence of light. Addition of one drop of dbu and 1 h further stirring ensured completion of reaction. The solution was filtered and the solvent removed *in vacuo*. The resultant dark red solid was dissolved in the minimum volume of CH_2Cl_2 and applied to an alumina chromatography column. The product was eluted as a red-purple band using CH_2Cl_2 and the solvent was removed to yield a bright red solid, *trans*-$[(C_5H_5)Fe(C_5H_4)C{\equiv}CRu(dppm)_2(C{\equiv}CR)]$ (0.8 mmol, 25%).

trans-$[(C_5H_5)Fe(C_5H_4)C{\equiv}CRu(dppm)_2(C{\equiv}CC_6H_4NO_2\text{-}4)]$ **2d** (Found: C, 67.9; H, 4.5; N, 1.0. $C_{70}H_{56}FeNO_2P_4Ru$ requires C, 68.7; H, 4.6; N, 1.1%): $\tilde{\nu}$/cm^{-1} (CH_2Cl_2) 2052 (C≡C); $\delta_H(CDCl_3)$ 3.63 (2 H, t), 3.92 (5 H, s), 4.10 (2 H, t), 4.81 (4 H, m) and 6.1–7.8 (44 H, m); $\delta_P(CDCl_3)$ −145.2; $\delta_C(CDCl_3)$ 52.0 (CH_2 of dppm), 65.6, 68.6, 68.9 (ferrocenyl C), 108 (C≡C) and 123–135 (Ph of dppm); *m/z* 1225.8 (M^+).

trans-$[(C_5H_5)Fe(C_5H_4)C{\equiv}CRu(dppm)_2(C{\equiv}CC_6H_3Me\text{-}3\text{-}NO_2\text{-}4)]$ **2e** (Found: C, 68.7; H, 4.8; N, 1.1. $C_{71}H_{58}FeNO_2P_4Ru$ requires C, 68.9; H, 4.7; N, 1.1%): $\tilde{\nu}$/cm^{-1} (CH_2Cl_2) 2047 (C≡C); $\delta_H(CDCl_3)$ 1.40 (3 H, s), 3.63 (2 H, t), 3.92 (5 H, s), 4.11 (2 H, t), 4.90 (4 H, m) and 5.8–7.3 (43 H, m); $\delta_P(CDCl_3)$ −145.0; $\delta_C(CDCl_3)$ 20.0 (C_6H_3*Me*), 52.0 (CH_2 of dppm), 65.4, 68.7, 68.9 (ferrocenyl C), 110 (C≡C) and 122–141 (Ph of dppm); *m/z* 1237.2 (M^+).

trans-$[(C_5H_5)Fe(C_5H_4)C{\equiv}CRu(dppm)_2(C{\equiv}C_6H_4NO_2\text{-}2)]$ **2f**: sample impure, efforts to purify failed; $\tilde{\nu}$/cm^{-1} (CH_2Cl_2) 2045 (C≡C); $\delta_H(CDCl_3)$ 3.63 (2 H, t), 3.92 (5 H, s), 4.10 (2 H, t), 4.87 (4 H, m) and 6.1–7.8 (44 H, m); $\delta_P(CDCl_3)$ −145.5; $\delta_C(CDCl_3)$ 52.0 (CH_2 of dppm), 65.2, 68.5, 68.9 (ferrocenyl C), 110 (C≡C) and 126–134 (Ph of dppm); *m/z* 1225.4 (M^+).

Table 5 Infrared and mass spectromeric data, and colours of the mixed-valence heterobimetallic complexes

Complex	IR $\tilde{\nu}(MCCCR_2)$/ cm^{-1}	Colour	Mass(calc.)	m/z [M^+(obs.)]
1a$^+$	1985	Blue	1113	1115
1b$^+$	1978	Blue	1203	1204
2a$^+$	1984, 2069, 2079*	Blue	1178	1180
2b$^+$	1984, 2065, 2074*	Blue	1254	1257
2c$^+$	1984, 2072, 2079*	Blue	1193	1195
2d$^+$	1990, 2068, 2081*	Brown	1224	1224
2g$^+$	1975, 2072	Blue	1286	1289

* Shoulder on previous peak.

Synthesis of mixed-valence heterobimetallic ferrocenyl complexes

The mixed-valence species **1a**$^+$,**1b**$^+$, **2a**$^+$–**2d**$^+$ and **2g**$^+$ were all synthesised by the same procedure. The complexes were characterised by colour, IR and mass spectra (Table 5). Complexes **1a**, **1b**, **2a**–**2d** and **2g** (0.1 mmol) were dissolved in CH_2Cl_2 (10 cm^3) under an argon atmosphere at 0 °C. Ferrocenium hexafluorophosphate (0.1 mmol) was added and the mixture stirred for 30 min. The solution was filtered and the solvent was removed. The resultant blue-purple powder was washed with diethyl ether to remove any $[Fe(C_5H_5)_2]$ by-product. The fine powder was then filtered off and dried *in vacuo*. The products were obtained in about 90% yield and were air-stable.

Acknowledgements

We thank the EPSRC and the British Council for financial support.

References

1 C. Kollmar, M. Couty and O. Kahn, *J. Am. Chem. Soc.*, 1991, **113**, 7994.
2 K. M. Chi, J. C. Calabrese, W. M. Reiff and J. S. Miller, *Organometallics*, 1991, **10**, 688.
3 R. W. Wagner, P. A. Brown, T. E. Johnson and J. S. Lindsey, *J. Chem. Soc., Chem. Commun.*, 1991, 1463.
4 E. C. Constable, *Angew. Chem., Int. Ed. Engl.*, 1991, **30**, 407.
5 I. R. Butler, *Organometallic Chemistry*, ed. E. W. Abel, Royal Society of Chemistry, Specialist Periodic Reports, 1992, vol. 21, p. 338.
6 S. R. Marder, *Inorganic Materials*, eds. D. W. Bruce and D. O'Hare, Wiley, Chichester, 1992, p. 136.
7 See, for example, K. L. Kott, D. A. Higgins, R. J. McMahon and R. M. Corn, *J. Am. Chem. Soc.*, 1993, **115**, 5342; Z. Yuan, N. J. Taylor, Y. Sun, T. B. Marder, I. D. Williams and L.-T. Cheng, *J. Organomet. Chem.*, 1993, **449**, 27; Z. Yuan, G. Stringer, I. R. Jobe, D. Kreller, K. Scott, L. Koch, N. J. Taylor and T. B. Marder, *J. Organomet. Chem.*, 1993, **452**, 115; A. Benito, J. Cano, R. Martinez-Manez, J. Paya, J. Soto, M. Julve, F. Lloret, M. D. Marcos and E. Sinn, *J. Chem. Soc., Dalton Trans.*, 1993, 1999.
8 J. C. Calabrese, L.-T. Cheng, J. C. Green, S. R. Marder and W. Tam, *J. Am. Chem. Soc.*, 1991, **113**, 7227.
9 C. C. Frazier, M. A. Harvey, M. P. Cockerham, H. M. Hand, E. A. Chauchard and C. H. Lee, *J. Phys. Chem.*, 1986, **90**, 5703.
10 N. J. Long, *Angew. Chem., Int. Ed. Engl.*, 1995, **34**, 21.
11 M. C. B. Colbert, S. L. Ingham, J. Lewis, N. J. Long and P. R. Raithby, *J. Chem. Soc., Dalton Trans.*, 1994, 2215.
12 D. Touchard, P. Haquette, N. Pirio, L. Toupet and P. H. Dixneuf, *Organometallics*, 1993, **12**, 3132.
13 (*a*) S. L. Ingham, M. S. Khan, J. Lewis, N. J. Long and P. R. Raithby, *J. Organomet. Chem.*, 1994, **470**, 153; (*b*) Z. Atherton, C. W. Faulkner, S. L. Ingham, A. K. Kakkar, M. S. Khan, J. Lewis, N. J. Long and P. R. Raithby, *J. Organomet. Chem.*, 1993, **462**, 265; (*c*) C. W. Faulkner, Ph.D. Thesis, University of Cambridge, 1994.
14 M. R. Torres, A. Santos, J. Ros and X. Solans, *Organometallics*, 1987, **6**, 1091; M. J. Tenorio, M. C. Puerta and P. Valerga, *J. Chem. Soc., Chem. Commun.*, 1993, 1750.
15 T. E. Müller, D. M. P. Mingos and D. J. Williams, *J. Chem. Soc., Chem. Commun.*, 1994, 1787.
16 M. Sato, H. Shintate, Y. Kawata, M. Sekino, M. Katada and S. Kawata, *Organometallics*, 1994, **13**, 1956.
17 N. Dowling, P. M. Henry, N. A. Lewis and H. Taube, *Inorg. Chem.*, 1981, **20**, 2345.
18 M. C. B. Colbert, Ph.D. Thesis, University of Cambridge, 1995.
19 S. B. Colbran, B. H. Robinson and J. Simpson, *Organometallics*, 1983, **2**, 943.
20 M. C. B. Colbert, J. Lewis, N. J. Long, N. A. Page, D. G. Parker, P. R. Raithby, D. A. Bloor and G. H. Cross, unpublished work.
21 G. C. Allen and N. S. Hush, *Prog. Inorg. Chem.*, 1967, **8**, 357.
22 M. B. Robin and P. Day, *Adv. Inorg, Chem. Radiochem.*, 1967, **10**, 247.
23 S. J. Lippard, *Prog. Inorg. Chem.*, 1983, **30**, 1.
24 D. F. Shriver, *Manipulation of Air-sensitive Compounds*, McGraw-Hill, New York, 1969.
25 SHELXTL PC, version 5.03, Siemens Analytical X-Ray Instruments, Madison, WI, 1990.
26 P. Haquette, N. Pirio, D. Touchard, L. Toupet and P. H. Dixneuf, *J. Chem. Soc., Chem. Commun.*, 1993, 163.

Received 24*th July* 1996; *Paper* 6/05177D